ELSEVIER

International Journal of Solids and Structures 41 (2004) 3865–3889

INTERNATIONAL JOURNAL OF SOLIDS and STRUCTURES

www.elsevier.com/locate/ijsolstr

Contact mechanics of graded coatings

M.A. Guler *, F. Erdogan

Department of Mechanical Engineering and Mechanics, Lehigh University, 19 Memorial Drive West, Bethlehem, PA 18015-3085, USA

Received 15 August 2003; received in revised form 10 February 2004
Available online 18 March 2004

Abstract

The main interest of this study is in the fracture initiation in graded coatings under sliding contact loading. The structural component under consideration is a metallic substrate bonded to a metal/ceramic coating with continuously varying thermo-mechanical properties. The coating is 100% ceramic at the free surface and 100% metal at the interface. It is assumed that the thickness variation of the shear modulus of the coating is exponential and the Poisson's ratio is constant. The loading is provided by a sliding rigid stamp subjected to constant normal and tangential forces and the underlying elasticity problem is two-dimensional. On the contact area, it is also assumed that the conditions of Coulomb friction prevail. The objective of the study is to obtain a series of analytical benchmark solutions for examining the influence of such factors as material inhomogeneity constants, the coefficient of friction and various length parameters on the critical stresses that may have a bearing on the fatigue and fracture of the coating.

Keywords: Contact mechanics; Functionally graded coatings; Friction

1. Introduction

Graded materials or functionally graded materials (FGMs) are multiphase composites with continuously varying volume fractions and, consequently, thermo-mechanical properties. Many of the present and potential applications of FGMs involve contact problems which are mostly load transfer problems in the presence of friction. Such structural components as bearings, gears, machine tools, cams and abradable seals in gas turbines may be mentioned as some examples (Trumble et al., 2000; Pan et al., 2003; Miyamoto et al., 1999). An important problem in the design of load transfer components is the preparation of surfaces to reduce the likelihood of cracking. Thus, the optimum design of these components requires the necessary material toughness and wear resistance near and at the surfaces. A simple solution to the problem may be coating the essentially metallic substrate by a ceramic layer. The shortcomings of this approach appear to be poor bonding strength, relatively high residual stresses and the brittleness of the surface layer. Replacing the ceramic coating by a metal/ceramic FGM layer seems to provide a way toward eliminating these

* Corresponding author. Tel.: +1-631-455-3372; fax: +1-610-758-6224.
E-mail address: maguler@yahoo.com (M.A. Guler).

0020-7683/$ - see front matter
doi:10.1016/j.ijsolstr.2004.02.025

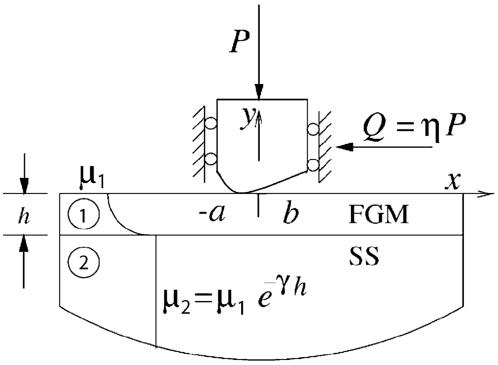

Fig. 1. Geometry of the contact problem.

shortcomings. The underlying somewhat simplified mechanics problem is then the following: A relatively thick homogeneous metallic substrate is coated by a metal/ceramic FGM layer in such a way that the layer is 100% ceramic at the surface and 100% metal at the interface (Fig. 1). The Poisson's ratio is constant throughout the medium and the shear modulus of the FGM coating is given by $\mu_c(y) = \mu_s \exp(\gamma y)$ where μ_s is the shear modulus of the substrate and γ is the material inhomogeneity constant. The composite medium is loaded by a sliding rigid stamp subjected to a normal force P and a tangential force $Q = \eta P$, where η is the coefficient of friction. The primary objective of the study is the determination of the stress components σ_{xx}, σ_{yy}, and σ_{xy} on the surface of the coating in order to examine the question of crack initiation (see, for example Lawn (1993) for surface cracking of glass under sliding spherical steel indenter and Suresh et al. (1999) for similar results for glass and polycrystalline alumina).

The related fundamental contact problem for the homogeneous materials is the Cattaneo's problem (see Hills et al. (1993) for the main results in contacting shallow cylinders and Ciavarella (1998a,b) for some recent results on the slip-stick problem). In this problem the normal force P is fixed and the tangential force Q increased monotonically from zero to ηP. The problem is one of partial slip or slip-stick for $0 \leqslant Q < \eta P$ and sliding contact for $Q = \eta P$.

Aside from the finite coating thickness an important feature of the contact problem considered in this study is the material inhomogeneity. The contact problem for inhomogeneous materials has only a limited number of solutions mostly by Suresh and coworkers. Suresh et al. (1997) studied the axisymmetric indentation problem for a graded medium with Young's modulus $E(z) = E_0 \exp(\alpha z)$ and spatially constant Poisson's ratio. It was assumed that the profile of the indenter is a parabola and the contact is frictionless. The results include the finite element solution, description of the experiments giving the load vs. indenter displacement and the comparison of the theory and experiments. The theoretical (by finite element technique) and experimental investigation of a graded medium loaded by a sliding spherical indenter and the resulting surface cracking was carried out by Suresh et al. (1999). The "metal" phase of the medium was polycrystalline alumina and the "ceramic" phase was alumina slicate glass. The depth variation of the modulus of the medium was assumed to be a power law of the form $E(z) = E_s + E_0 z^k$ where E_s is the surface value, $0 < k < 1$ and the constant E_0 is selected in such a way that the units are consistent.

The axisymmetric graded half space problem for a concentrated load and for flat, spherical and conical indenters were considered by Giannakopoulos and Suresh (1997a,b). In these studies, too it was assumed that the Poisson's ratio is constant and the Young's modulus varies in depth direction either as a simple power law ($E(z) = E_0 z^k$, $0 \leqslant k < 1$) or exponentially ($E(z) = E_0 e^{\alpha z}$) and the contact is frictionless. Dag and Erdogan (2002) considered the coupled plane strain problem of crack/contact mechanics for an inhomogeneous medium with spatially constant Poisson's ratio and exponentially varying Young's modulus

$E(x) = E_s \exp(\gamma x)$, E_s being the surface value and x the depth coordinate. In the sliding contact problem studied it was shown that the trailing end of the stamp has higher stress concentration (for the case of smooth contact) or higher stress singularity (for the case of flat stamps), the stress singularity depends on the coefficient of friction and the surface value of the Poisson's ratio and is independent of the inhomogeneity constant γ and the Young's modulus as long as E_s is non zero. It should be emphasized that for small values of x, since any variation of $E(x)$ can locally be represented by $E_0 \exp(\gamma x)$, for the same coefficient of friction and the same Poisson's ratio, the stress singularities are the same for a homogeneous and an inhomogeneous sliding contact problems.

An approximate solution of the plane strain sliding contact problem for a rigid cylindrical stamp acting on a graded medium is given by Giannakopoulos and Pallot (2000). The Young's modulus of the (semi-infinite) graded medium is assumed to be $E(y) = E_0 y^k$, $0 \leqslant k \leqslant 1$ (see, also Booker et al., 1985). Since it is rather difficult to think of materials with vanishing stiffness on the surface, at best results are approximate. As indicated in the forgoing discussion, with a nonvanishing Young's modulus on the surface the stress singularity for a flat stamp is independent of material inhomogeneity (in this case k) and is dependent only on the surface value of the Poisson's ratio and the coefficient of friction. In this sense the heavy dependence of the singularity on the inhomogeneity constant k as shown in Eq. (25) does not seem to be physically acceptable. The sliding contact problem for a graded medium was also considered by Guler and Erdogan (1998). In the plane strain problem studied it was assumed that the Young's modulus varies exponentially in depth direction and the rigid stamp may be flat, parabolic, semi circular or wedge-shaped. The sliding contact problem for a graded coating bonded to a homogeneous substrate is considered in this study.

2. The formulation of FGM-coated elastic half plane

Consider the plane elasticity problem show in Fig. 2. Medium 2 is a homogeneous substrate and medium 1 is the graded coating with a thickness h. The shear moduli of the coating and substrate are given by $\mu(y)$ and μ_2 respectively. μ_2 is constant and $\mu(y)$ is approximated by

$$\mu(y) = \mu_1 e^{\gamma y}, \quad -h < y < 0, \tag{1}$$

where γ is a constant characterizing the material inhomogeneity, μ_1 is the value of $\mu(y)$ at the surface and μ_1 and μ_2 are related by

$$\mu_2 = \mu_1 e^{-\gamma h}. \tag{2}$$

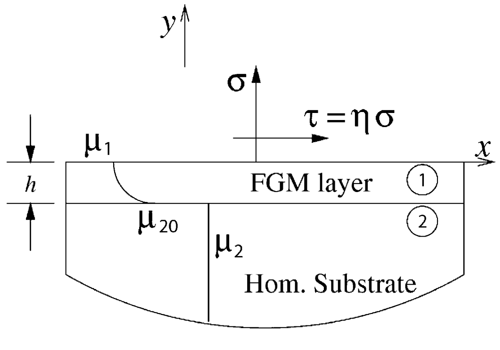

Fig. 2. Geometry of the problem for an FGM-coated homogeneous half plane.

Defining

$$\Gamma_3 = \frac{\mu_2}{\mu_1} \tag{3}$$

for future reference, from (2) and (3) γ may be expressed as

$$\gamma = -\frac{1}{h}\log\Gamma_3. \tag{4}$$

In the composite medium $-\infty < y < 0$ the spatial variation of the Poisson's ratio is assumed to be negligible. Thus, we have $v_2 = v_1(y) = v = \text{constant}$.

For the plane contact problem under consideration the Hooke's law in the region $-h < y < 0$ can be written as

$$\sigma_{1xx}(x,y) = \frac{\mu(y)}{\kappa - 1}\left[(\kappa+1)\frac{\partial u_1}{\partial x} + (3-\kappa)\frac{\partial v_1}{\partial y}\right], \tag{5a}$$

$$\sigma_{1yy}(x,y) = \frac{\mu(y)}{\kappa - 1}\left[(3-\kappa)\frac{\partial u_1}{\partial x} + (\kappa+1)\frac{\partial v_1}{\partial y}\right], \tag{5b}$$

$$\sigma_{1xy}(x,y) = \mu_1(y)\left[\frac{\partial u_1}{\partial y} + \frac{\partial v_1}{\partial x}\right], \tag{5c}$$

where $\kappa = 3 - 4v$ for plane strain and $\kappa = (3-v)/(1+v)$ for the generalized plane stress conditions. For medium 2, $-\infty < y < -h$, μ_2 replaces $\mu(y)$ in (5).

Substituting (5) into the equilibrium equations we obtain

$$(\kappa+1)\frac{\partial^2 v_1}{\partial y^2} + (\kappa-1)\frac{\partial^2 v_1}{\partial x^2} + 2\frac{\partial^2 u_1}{\partial x \partial y} + \gamma(3-\kappa)\frac{\partial u_1}{\partial x} + \gamma(\kappa+1)\frac{\partial v_1}{\partial y} = 0, \quad -h < y < 0, \tag{6a}$$

$$(\kappa+1)\frac{\partial^2 u_1}{\partial x^2} + (\kappa-1)\frac{\partial^2 u_1}{\partial y^2} + 2\frac{\partial^2 v_1}{\partial x \partial y} + \gamma(\kappa-1)\frac{\partial u_1}{\partial y} + \gamma(\kappa-1)\frac{\partial v_1}{\partial x} = 0, \quad -h < y < 0, \tag{6b}$$

$$(\kappa+1)\frac{\partial^2 u_2}{\partial x^2} + (\kappa-1)\frac{\partial^2 u_2}{\partial y^2} + 2\frac{\partial^2 v_2}{\partial x \partial y} = 0, \quad -\infty < y < -h, \tag{7a}$$

$$(\kappa+1)\frac{\partial^2 v_2}{\partial y^2} + (\kappa-1)\frac{\partial^2 v_2}{\partial x^2} + 2\frac{\partial^2 u_2}{\partial x \partial y} = 0, \quad -\infty < y < -h. \tag{7b}$$

By using the Fourier transforms, the displacement components, $u_1(x,y)$, $v_1(x,y)$, $u_2(x,y)$ and $v_2(x,y)$ may be expressed as

$$u_1(x,y) = \frac{1}{2\pi}\int_{-\infty}^{\infty} F_1(\alpha,y)e^{i\alpha x}\,d\alpha, \qquad v_1(x,y) = \frac{1}{2\pi}\int_{-\infty}^{\infty} G_1(\alpha,y)e^{i\alpha x}\,d\alpha, \tag{8a, b}$$

$$u_2(x,y) = \frac{1}{2\pi}\int_{-\infty}^{\infty} F_2(\alpha,y)e^{i\alpha x}\,d\alpha, \qquad v_2(x,y) = \frac{1}{2\pi}\int_{-\infty}^{\infty} G_2(\alpha,y)e^{i\alpha x}\,d\alpha, \tag{9a, b}$$

$$F_1(\alpha,y) = \sum_{j=5}^{8} A_{5j}(\alpha)e^{n_j y}, \qquad G_1(\alpha,y) = \sum_{j=5}^{8} A_{6j}(\alpha)e^{n_j y}, \tag{10a, b}$$

$$F_2(\alpha,y) = [A_{75}(\alpha) + A_{76}(\alpha)y]e^{|\alpha|y} + [A_{77}(\alpha) + A_{78}(\alpha)y]e^{-|\alpha|y}, \tag{11a}$$

$$G_2(\alpha,y) = [A_{85}(\alpha) + A_{86}(\alpha)y]e^{|\alpha|y} + [A_{87}(\alpha) + A_{88}(\alpha)y]e^{-|\alpha|y}, \tag{11b}$$

where n_j $(j = 5,\ldots,8)$ satisfies the following characteristic equation

$$(n_j^2 - \alpha^2 + \gamma n_j)^2 + \delta^2|\alpha|^2|\gamma|^2 = 0, \tag{12}$$

$$n_5 = \frac{1}{2}\Big(-\gamma + \sqrt{\gamma^2 + 4(\alpha^2 + i|\alpha||\gamma|\delta)}\Big), \tag{13a}$$

$$n_6 = \frac{1}{2}\Big(-\gamma - \sqrt{\gamma^2 + 4(\alpha^2 + i|\alpha||\gamma|\delta)}\Big), \tag{13b}$$

$$n_7 = \frac{1}{2}\Big(-\gamma + \sqrt{\gamma^2 + 4(\alpha^2 - i|\alpha||\gamma|\delta)}\Big), \tag{13c}$$

$$n_8 = \frac{1}{2}\Big(-\gamma - \sqrt{\gamma^2 + 4(\alpha^2 - i|\alpha||\gamma|\delta)}\Big), \tag{13d}$$

$$\delta^2 = \frac{3-\kappa}{\kappa+1}. \tag{13e}$$

The functions $A_{5j}(\alpha)$, $A_{6j}(\alpha)$, $A_{7j}(\alpha)$ and $A_{8j}(\alpha)$ $(j = 5,\ldots,8)$ are unknown and are not independent. The relationship between them can be written as

$$A_{75}(\alpha) = i\left[\frac{|\alpha|}{\alpha}A_{85}(\alpha) + \frac{\kappa}{\alpha}A_{86}(\alpha)\right], \quad A_{76}(\alpha) = i\frac{|\alpha|}{\alpha}A_{86}(\alpha), \tag{14a, b}$$

$$A_{77}(\alpha) = i\left[-\frac{|\alpha|}{\alpha}A_{87}(\alpha) + \frac{\kappa}{\alpha}A_{88}(\alpha)\right], \quad A_{78}(\alpha) = -i\frac{|\alpha|}{\alpha}A_{88}(\alpha), \tag{15a, b}$$

$$A_{5j}(\alpha) = a_j(\alpha)A_{6j}(\alpha), \quad j = 5,6, \quad A_{5j}(\alpha) = -\bar{a}_{j-2}(\alpha)A_{6j}(\alpha), \quad j = 7,8, \tag{16a, b}$$

$$a_j(\alpha) = -\frac{(\kappa+1)\left(n_j^2 + \gamma n_j\right) - (\kappa-1)\alpha^2}{i\alpha[2n_j + \gamma(3-\kappa)]}, \quad j = 5,\ldots,8. \tag{17}$$

In the formulation given above, there are a total of eight unknowns, A_{6j} and A_{8j} $(j = 5,\ldots,8)$. The boundedness of σ_{2yy} and σ_{2xy} as $|x^2 + y^2| \to \infty$ requires that A_{87} and A_{88} be zero. The remaining six unknowns are obtained from the following continuity and boundary conditions on the surface of the coating

$$u_1(x,-h) = u_2(x,-h), \qquad v_1(x,-h) = v_2(x,-h), \tag{18a, b}$$

$$\sigma_{1yy}(x,-h) = \sigma_{2yy}(x,-h), \qquad \sigma_{1xy}(x,-h) = \sigma_{2xy}(x,-h), \tag{19a, b}$$

$$\sigma_{1yy}(x,0) = \sigma(x), \qquad \sigma_{1xy}(x,0) = \tau(x). \tag{20a, b}$$

Of the six unknowns four may be eliminated by using four homogeneous conditions (18) and (19). The remaining two unknowns (A_{65}, A_{67}) may then be expressed by using (20) as follows:

$$A_{65} = -\frac{1}{\mu_1\Delta_5}[(\kappa-1)P(\alpha)\bar{r}_8 + \bar{r}_6 Q(\alpha)], \tag{21a}$$

$$A_{67} = -\frac{1}{\mu_1 \Delta_5}[r_6 Q(\alpha) - (\kappa - 1)P(\alpha)r_8], \tag{21b}$$

where Δ_5, r_6 and r_8 are known functions and P and Q are given by (see Guler (2001) for details)

$$P(\alpha) = \int_{-\infty}^{\infty} \sigma(t)\mathrm{e}^{-\mathrm{i}\alpha t}\,\mathrm{d}t, \qquad Q(\alpha) = \int_{-\infty}^{\infty} \tau(t)\mathrm{e}^{-\mathrm{i}\alpha t}\,\mathrm{d}t. \tag{22a, b}$$

3. Integral equation for the stamp problem

The formulation given in the previous section describes the solution of the ordinary stress boundary value problem shown in Fig. 2. On the other hand the contact problems shown in Figs. 1 and 3 for a rigid stamp are mixed boundary value problems in which the tractions σ and τ are known to be zero outside the contact region and within the contact region $-a < x < b$ the displacement components are known through the given stamp profile. By using the derivation described in Section 2 the displacements on the surface may be expressed as

$$\lim_{y\to 0} 2\pi\mu_1 \frac{\partial}{\partial x} v_1(x,y) = \lim_{y\to 0} \int_{-a}^{b} K_{11}(x,y,t)\sigma(t)\,\mathrm{d}t + \lim_{y\to 0} \int_{-a}^{b} K_{12}(x,y,t)\tau(t)\,\mathrm{d}t, \tag{23a}$$

$$\lim_{y\to 0} 2\pi\mu_1 \frac{\partial}{\partial x} u_1(x,y) = \lim_{y\to 0} \int_{-a}^{b} K_{21}(x,y,t)\tau(t)\,\mathrm{d}t + \lim_{y\to 0} \int_{-a}^{b} K_{22}(x,y,t)\sigma(t)\,\mathrm{d}t, \tag{23b}$$

where the kernels K_{ij} are known functions (see Guler (2001) for details) and to dictate the nature of singularity of the resulting integral equations (in this case Cauchy singularities and delta functions) (23) is expressed in terms of displacement derivatives rather than displacements. We now observe that the kernels K_{ij} are of the form

$$K_{ij}(x,y,t) = \int_{-\infty}^{\infty} h_{ij}(y,\alpha)\mathrm{e}^{-\mathrm{i}\alpha(t-x)}\,\mathrm{d}\alpha, \quad (i = 1,2;\ j = 1,2). \tag{24}$$

Thus examining the asymptotic behavior of h_{ij} for $|\alpha| \to \infty$, the leading terms in (24) may be obtained as (see Guler (2001) for details)

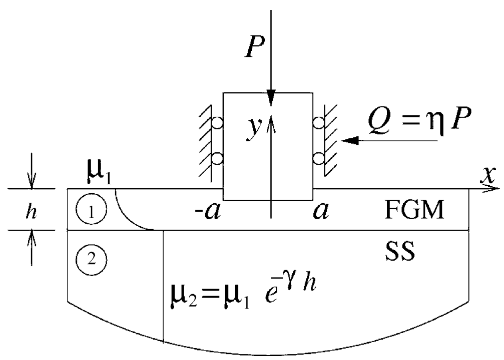

Fig. 3. Geometry of the flat stamp problem.

$$K_{11\infty}(x,y,t) = K_{21\infty}(x,y,t) = \frac{\kappa+1}{4}\int_{-\infty}^{\infty}\frac{\mathrm{i}|\alpha|}{\alpha}\mathrm{e}^{|\alpha|y}\mathrm{e}^{-\mathrm{i}\alpha(t-x)}\,\mathrm{d}\alpha = \frac{\kappa+1}{4}\frac{2(t-x)}{(t-x)^2-y^2}, \quad y<0, \tag{25}$$

$$K_{12\infty}(x,y,t) = -K_{22\infty}(x,y,t) = -\frac{\kappa-1}{4}\int_{-\infty}^{\infty}\mathrm{e}^{|\alpha|y}\mathrm{e}^{-\mathrm{i}\alpha(t-x)}\,\mathrm{d}\alpha = -\frac{\kappa-1}{4}\frac{2y}{(t-x)^2+y^2}, \quad y<0. \tag{26}$$

By using the limits

$$\lim_{y\to 0^-}\frac{t-x}{(t-x)^2+y^2} = \frac{1}{t-x}, \qquad \lim_{y\to 0^-}\frac{y}{(t-x)^2+y^2} = -\pi\delta(t-x) \tag{27a, b}$$

from (23) it follows that

$$-\omega\tau(x) + \frac{1}{\pi}\int_{-a}^{b}\left[\frac{1}{t-x} - k_{11}(t,x)\right]\sigma(t)\,\mathrm{d}t - \frac{1}{\pi}\int_{-a}^{b}\tau(t)k_{12}(t,x)\,\mathrm{d}t = f(x), \quad -a<x<b, \tag{28a}$$

$$\omega\sigma(x) + \frac{1}{\pi}\int_{-a}^{b}\left[\frac{1}{t-x} - k_{21}(t,x)\right]\tau(t)\,\mathrm{d}t - \frac{1}{\pi}\int_{-a}^{b}\sigma(t)k_{22}(t,x)\,\mathrm{d}t = g(x), \quad -a<x<b, \tag{28b}$$

where the kernels k_{ij} are known bounded functions and

$$f(x) = \lambda\frac{\partial}{\partial x}v_1(x,0), \quad g(x) = \lambda\frac{\partial}{\partial x}u_1(x,0), \quad \lambda = \frac{4\mu_1}{\kappa+1}, \quad \omega = \frac{\kappa-1}{\kappa+1}. \tag{29a–d}$$

The expressions (28) constitute a pair of integral equations for the unknown contact stresses σ and τ, provided the stamp profile, that is, $u_1(x,0)$ and $v_1(x,0)$, $-a<x<b$ and the contact conditions (for example, perfect adhesion) are prescribed. In this study it is assumed that the stamp moves relative to the substrate, the coefficient of friction η in the contact region is constant and the friction is one of Coulomb type. Thus in the contact region we have

$$\sigma_{1yy}(x,0) = \sigma(x) = -p(x), \quad -a<x<b, \tag{30a}$$

$$\sigma_{1xy}(x,0) = \tau(x) = -\eta p(x), \quad -a<x<b, \tag{30b}$$

$p(x)$, $-a<x<b$, is the only unknown function and may be obtained from

$$\omega\eta p(x) + \frac{1}{\pi}\int_{-a}^{b}\left[-\frac{1}{t-x} + k_{11}(t,x) + \eta k_{12}(t,x)\right]p(t)\,\mathrm{d}t = f(x), \quad -a<x<b. \tag{31}$$

For a complete solution of the problem some additional conditions are needed. First, the contact pressure $p(x)$ must satisfy

$$\int_{-a}^{b}p(t)\,\mathrm{d}t = P, \tag{32}$$

where P is the resultant compressive force. The amplitude of the applied load may be given in terms of either P or stamp displacement v_0 parallel to the y-axis. Secondly, at the end points $-a$ and/or b if the contact is smooth (e.g. Fig. 1), then the solution $p(x)$ must also satisfy certain consistency conditions (Guler, 2001).

Detailed examination of the kernels in (31) shows that, in addition to the singular terms $1/(t-x)$ and $\delta(t-x)$, the kernels k_{11} and k_{12} have the following ill-behaved components which, for accuracy, needs to be treated separately in the numerical analysis.

$$k_{11\infty}(x,t) = -\frac{\kappa+5}{\kappa+1}\gamma\frac{\pi}{4}\frac{|t-x|}{t-x}, \tag{33a}$$

$$k_{12\infty}(x,t) = -\frac{\gamma}{2}\log\left|\frac{2(t-x)}{b+a}\right|. \tag{33b}$$

By defining the following normalized quantities

$$x = \frac{b+a}{2}r + \frac{b-a}{2}, \quad t = \frac{b+a}{2}s + \frac{b-a}{2}, \quad -a < (x,t) < b, \quad -1 < (r,s) < 1, \tag{34}$$

$$p(x) = \lambda\phi(r), \quad f(x) = \lambda F(r), \quad \omega\eta = A, \tag{35}$$

the integral equation (31) may be expressed in the following form

$$A\phi(r) - \frac{1}{\pi}\int_{-1}^{1}\frac{\phi(s)}{s-r}\,\mathrm{d}s + \frac{1}{\pi}\int_{-1}^{1}k(r,s)\phi(s)\,\mathrm{d}s = F(r), \quad -1 < r < 1, \tag{36}$$

where the kernel $k(r,s)$ is given by

$$k(r,s) = [k_{11}(x,t) + \eta k_{12}(x,t)]\frac{b+a}{2}. \tag{37}$$

4. On the solution of integral equations

For an accurate and efficient solution of the integral equation the corresponding weight function $w(s)$ needs to be determined. By defining the complex potential

$$\Phi(z) = \frac{1}{2\pi\mathrm{i}}\int_{-1}^{1}\frac{\phi(s)}{s-z}\,\mathrm{d}s \tag{38}$$

and using the complex function theory (Muskhelishvili, 1953), from the dominant part of the integral equation

$$\omega\eta\phi(r) - \frac{1}{\pi}\int_{-1}^{1}\frac{\phi(s)}{s-r}\,\mathrm{d}s = G(r), \tag{39}$$

the weight function of $\phi(s)$ may be determined as

$$w(s) = (1-s)^{\alpha}(1+s)^{\beta}, \quad -1 < s < 1, \tag{40}$$

$$\alpha = \frac{\theta}{\pi} + N_0, \quad \beta = -\frac{\theta}{\pi} + M_0, \quad \theta = \arctan\frac{1}{\omega\eta}, \tag{41}$$

where N_0 and M_0 are arbitrary (positive, zero or negative) integers and are determined from the physics of the problem. In (39) $G(r)$ represents all the bounded terms in (36).

After determining $w(s)$ the solution of (36) may be expressed as

$$\phi(s) = \sum_{n=0}^{\infty} c_n w(s) P_n^{(\alpha,\beta)}(s), \quad -1 < s < 1, \tag{42}$$

where c_n are unknown coefficients and $P_n^{(\alpha,\beta)}(s)$ are Jacobi polynomials associated with the weight function $w(s)$. By substituting (42) into (36) it may be shown that

$$\sum_{n=0}^{\infty} c_n \left[\frac{2^{-\kappa_0}}{\sin \pi\alpha} P_{n-\kappa_0}^{(-\alpha,-\beta)}(r) + K_n(r) \right] = F(r), \quad -1 < r < 1, \tag{43}$$

$$K_n(r) = \frac{1}{\pi} \int_{-1}^{1} k(r,s) P_n^{(\alpha,\beta)}(s) w(s)\, \mathrm{d}s, \quad \kappa_0 = -(\alpha + \beta), \tag{44}$$

where κ_0 is the index of the integral equation (Muskhelishvili, 1953).

The functional equation (43) can be reduced to a system of algebraic equations in c_n through a suitable collocation technique (Erdogan and Gupta, 1972). In the numerical solution of (43), higher accuracy is obtained when the density of the collocation points is increased near the ends by choosing the collocation points (r_i, $i = 0, 1, \dots, N$) as the roots of the Jacobi polynomials depending on the index of the problem.

5. The in-plane stress σ_{1xx} on the surface

Once the contact stresses $\sigma_{1yy}(x,0) = \sigma(x)$ and $\sigma_{1xy}(x,0) = \tau(x)$ are obtained, the in-plane stress $\sigma_{1xx}(x,0)$ on the surface of the FGM coating may be evaluated. By using the Hooke's law

$$\sigma_{1xx}(x,y) = \frac{\mu_1 \mathrm{e}^{\gamma y}}{\kappa - 1} \left[(\kappa + 1) \frac{\partial u_1}{\partial x} + (3 - \kappa) \frac{\partial v_1}{\partial y} \right], \tag{45}$$

$$\sigma_{1yy}(x,y) = \frac{\mu_1 \mathrm{e}^{\gamma y}}{\kappa - 1} \left[(3 - \kappa) \frac{\partial u_1}{\partial x} + (\kappa + 1) \frac{\partial v_1}{\partial y} \right], \tag{46}$$

$$\sigma_{1xy}(x,y) = \mu_1 \mathrm{e}^{\gamma y} \left[\frac{\partial u_1}{\partial y} + \frac{\partial v_1}{\partial x} \right] \tag{47}$$

and referring to (28) and (29), it may be shown that

$$\sigma_{1xx}(x,0) = \sigma_{1xx}^{p}(x,0) + \sigma_{1xx}^{q}(x,0), \tag{48}$$

$$\sigma_{1xx}^{p}(x,0) = \sigma(x) - \frac{2}{\pi} \int_{-a}^{b} k_{22}(t,x) \sigma(t)\, \mathrm{d}t, \tag{49a}$$

$$\sigma_{1xx}^{q}(x,0) = \frac{2}{\pi} \int_{-a}^{b} \left[\frac{1}{t - x} - k_{21}(t,x) \right] \tau(t)\, \mathrm{d}t. \tag{49b}$$

6. Examples

6.1. Flat stamp

Consider the contact problem for an FGM layer bonded to a homogeneous substrate shown in Fig. 3 where the stamp profile is given by

$$v_1(x,0) = -v_0 = \text{constant}, \quad \frac{\partial}{\partial x} v_1(x,0) = 0. \tag{50}$$

Referring to Fig. 3, (29) and (35), the integral equation (36) and the equilibrium equation (32) become

$$A\phi(r) + \frac{1}{\pi}\int_{-1}^{1}\left[-\frac{1}{s-r} + k(r,s)\right]\phi(s)\,\mathrm{d}s = 0, \tag{51}$$

$$\int_{-1}^{1}\phi(s)\,\mathrm{d}s = \frac{P}{\lambda a}. \tag{52}$$

The function $p(x)$ has integrable singularities at $x = a$ and $x = -a$. Thus, from the physics of the problem we must require that both α and β be negative. They may then be obtained by letting $N_0 = -1$ and $M_0 = 0$ as follows:

$$\begin{aligned} &\eta > 0: \quad \alpha = -1 + \frac{\theta}{\pi}, \quad \beta = -\frac{\theta}{\pi}, \\ &\eta = 0: \quad \alpha = -0.5, \quad \beta = -0.5, \\ &\eta < 0: \quad \alpha = -\frac{\theta}{\pi}, \quad \beta = -1 + \frac{\theta}{\pi}, \end{aligned} \tag{53}$$

where

$$\theta = \arctan\left|\frac{\kappa+1}{\eta(\kappa-1)}\right|, \quad 0 < \theta < \frac{\pi}{2}. \tag{54}$$

Assuming a solution of the form (42), using the properties of Jacobi Polynomials and truncating the series at N, Eq. (43) becomes

$$\sum_{n=0}^{N} c_n\left[\frac{1}{2\sin\pi\alpha}P_{n-1}^{(-\alpha,-\beta)}(r) + K_n(r)\right] = 0, \quad -1 < r < 1. \tag{55}$$

By using the collocation technique (55) gives N equations for $N+1$ unknown constants $c_0,\ldots,c_N$. The additional equation for a unique solution is provided by the equilibrium condition (52) which becomes

$$\sum_{n=0}^{N} c_n^* \int_{-1}^{1} w(s)P_n^{(\alpha,\beta)}(s)\,\mathrm{d}s = 1, \tag{56}$$

where

$$c_n^* = \frac{\lambda a}{P}c_n. \tag{57}$$

Using the following orthogonality condition

$$\int_{-1}^{1} P_n^{(\alpha,\beta)}(t)P_j^{(\alpha,\beta)}(t)w(t)\,\mathrm{d}t = \begin{cases} 0, & n \neq j, \\ \theta_j^{(\alpha,\beta)}, & n = j, \end{cases} \quad j = 0,1,2,\ldots, \tag{58}$$

where

$$\theta_0^{(\alpha,\beta)} = \int_{-1}^{1} w(t)\,\mathrm{d}t = \frac{2^{\alpha+\beta+1}\Gamma(\alpha+1)\Gamma(\beta+1)}{\Gamma(\alpha+\beta+2)}, \tag{59}$$

$$\theta_j^{(\alpha,\beta)} = \frac{2^{\alpha+\beta+1}\Gamma(j+\alpha+1)\Gamma(j+\beta+1)}{(2j+\alpha+\beta+1)j!\Gamma(j+\alpha+\beta+1)}, \tag{60}$$

we obtain the following $N+1$ equations

$$c_0^*\theta_0 = 1, \quad \sum_{n=1}^{N} c_n^* F_n(r_i) = 0, \quad i = 1, \ldots, N, \tag{61a, b}$$

where

$$F_n(r_i) = \frac{1}{2\sin\pi\alpha} P_{n-1}^{(-\alpha,-\beta)}(r_i) + K_n(r_i). \tag{62}$$

In (62) r_i ($i = 1, \ldots, N$) are obtained by letting

$$P_N^{(\alpha+1,\beta+1)}(r_i) = 0, \quad i = 1, \ldots, N. \tag{63}$$

After determining c_n, the contact stresses and the in-plane stress may be obtained as

$$\frac{\sigma_{1yy}(x,0)}{\sigma_0} = -\frac{p(x)}{\sigma_0}, \tag{64a}$$

$$\frac{\sigma_{1xy}(x,0)}{\sigma_0} = -\eta\frac{p(x)}{\sigma_0}, \tag{64b}$$

$$\frac{\sigma_{1xx}(x,0)}{\sigma_0} = -\frac{p(x)}{\sigma_0} - \frac{2\eta}{\pi\sigma_0}\int_{-a}^{a}\frac{p(t)}{t-x}\,\mathrm{d}t + \frac{2}{\pi\sigma_0}\int_{-a}^{a}[k_{22}(t,x) + \eta k_{21}(t,x)]p(t)\,\mathrm{d}t, \tag{64c}$$

$$\sigma_0 = \frac{P}{2a}, \tag{64d}$$

where

$$p(x) = 2\sigma_0\left(1-\frac{x}{a}\right)^{\alpha}\left(1+\frac{x}{a}\right)^{\beta}\sum_{n=0}^{N} c_n^* P_n^{(\alpha,\beta)}\left(\frac{x}{a}\right). \tag{65}$$

Upon solving the problem, the stress intensity factors at the end points $x = \pm a$ of the flat stamp may be defined as and evaluated from

$$k_1(a) = \lim_{x\to a}\frac{p(x)}{2^{\beta}(a-x)^{\alpha}} = \frac{2\sigma_0}{a^{\alpha}}\sum_{n=0}^{N} c_n^* P_n^{(\alpha,\beta)}(1), \tag{66a}$$

$$k_1(-a) = \lim_{x\to a}\frac{p(x)}{2^{\alpha}(x+a)^{\beta}} = \frac{2\sigma_0}{a^{\beta}}\sum_{n=0}^{N} c_n^* P_n^{(\alpha,\beta)}(-1). \tag{66b}$$

6.2. Triangular stamp

Consider now the stamp problem for the FGM layer bonded to a homogeneous substrate shown in Fig. 4 where the stamp profile is given by

$$v_1(x,0) = mx + C, \quad \frac{\partial}{\partial x}v_1(x,0) = m, \tag{67}$$

where m is a positive constant.

Defining

$$x = \frac{b}{2}(r+1), \quad t = \frac{b}{2}(s+1), \quad p(t) = \lambda\phi(s), \tag{68}$$

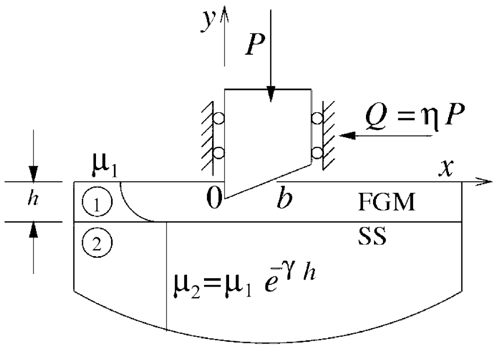

Fig. 4. Geometry of the triangular stamp problem.

the integral equation (36) and the equilibrium condition (32) become

$$A\phi(r) + \frac{1}{\pi}\int_{-1}^{1}\left[-\frac{1}{s-r} + k(r,s)\right]\phi(s)\,\mathrm{d}s = m, \tag{69}$$

$$\int_{-1}^{1}\phi(s)\,\mathrm{d}s = \frac{2P}{\lambda b}. \tag{70}$$

Since the triangular stamp has a sharp corner at $x = 0$, and smooth contact at $x = b$, from the physics of the problem it follows that α be positive and β be negative. They can then be found by letting $N_0 = M_0 = 0$ in (41) as

$$\begin{aligned} &\eta > 0: \quad \alpha = \frac{\theta}{\pi}, \quad \beta = -\frac{\theta}{\pi}, \\ &\eta = 0: \quad \alpha = 0.5, \quad \beta = -0.5, \\ &\eta < 0: \quad \alpha = 1 - \frac{\theta}{\pi}, \quad \beta = -1 + \frac{\theta}{\pi}, \end{aligned} \tag{71}$$

where θ is given by Eq. (41).

Assuming a solution of the form (42) and using the properties of Jacobi Polynomials and truncating the series at N, Eq. (43) becomes

$$\sum_{n=0}^{N} c_n^*\left[\frac{1}{\sin\pi\alpha}P_n^{(-\alpha,-\beta)}(r) + K_n(r)\right] = 1, \quad -1 < r < 1, \tag{72a}$$

$$c_n^* = \frac{c_n}{m}. \tag{72b}$$

In this problem, after the application of the load P, one end of the contact length, namely b is unknown. However, for a given value of the contact length, Eq. (72) provides $N + 1$ equations for $N + 1$ unknown constants $(c_0, \ldots, c_N)$ as follows:

$$\sum_{n=0}^{N} c_n^*\left[\frac{1}{\sin\pi\alpha}P_n^{(-\alpha,-\beta)}(r_i) + K_n(r_i)\right] = 1, \quad i = 1, \ldots, N+1, \; -1 < r < 1, \tag{73}$$

where r_i $(i = 1, \dots, N+1)$ are defined by

$$P_{N+1}^{(\alpha-1,\beta+1)}(r_i) = 0, \quad r_i \ (i = 1, \dots, N+1). \tag{74}$$

The relationship between the applied load P and the contact length, b can be found from the equilibrium equation (70) which becomes:

$$c_0^* \theta_0 = \frac{2P}{\lambda b m}, \tag{75}$$

where θ_0 can be computed from Eq. (59)

$$\theta_0 = \frac{2\pi\alpha}{\sin \pi\alpha}, \tag{76}$$

$$\frac{P}{\mu_1 m} = \frac{2c_0^*\theta_0}{\kappa+1} b. \tag{77}$$

The contact stresses and the in-plane stress in nondimensional form at the surface of the FGM coating can then be expressed as

$$\frac{\sigma_{1yy}(x,0)}{\mu_1 m} = -\frac{p(x)}{\mu_1 m}, \tag{78a}$$

$$\frac{\sigma_{1xy}(x,0)}{\mu_1 m} = -\eta\frac{p(x)}{\mu_1 m}, \tag{78b}$$

$$\frac{\sigma_{1xx}(x,0)}{\mu_1 m} = -\frac{p(x)}{\mu_1 m} - \frac{2\eta}{\pi\mu_1 m}\int_0^b \frac{p(t)}{t-x}\,\mathrm{d}t + \frac{2}{\pi\mu_1 m}\int_0^b [k_{22}(t,x) + \eta k_{21}(t,x)]p(t)\,\mathrm{d}t, \tag{78c}$$

where

$$p(x) = \frac{4\mu_1 m}{\kappa+1}\left(\frac{b-x}{x}\right)^{\alpha}\sum_{n=0}^{N} c_n^* P_n^{(\alpha,\beta)}\left(\frac{2x}{b}-1\right). \tag{79}$$

After determining c_n^* the stress intensity factor at $x = 0$ may be defined as and obtained from

$$k_1(0) = \lim_{x\to 0} x^{\alpha} p(x) = \frac{4\mu_1 m b^{\alpha}}{\kappa+1}\sum_{n=0}^{N} c_n^* P_n^{(\alpha,\beta)}(-1). \tag{80}$$

Table 1
Stress intensity factors for flat stamp $a/h = 0.1$, $\Gamma_3 = \mu_2/\mu_1$ (Fig. 3)

Γ_3	$\eta = 0.0$, $\alpha = -0.5$, $\beta = -0.5$	$\eta = 0.1$, $\alpha = -0.5091$, $\beta = -0.4909$		$\eta = 0.3$, $\alpha = -0.5272$, $\beta = -0.4728$		$\eta = 0.5$, $\alpha = -0.5452$, $\beta = -0.4548$	
	$\frac{k_1(a)}{Pa^{\beta}}$	$\frac{k_1(-a)}{Pa^{\alpha}}$	$\frac{k_1(a)}{Pa^{\beta}}$	$\frac{k_1(-a)}{Pa^{\alpha}}$	$\frac{k_1(a)}{Pa^{\beta}}$	$\frac{k_1(-a)}{Pa^{\alpha}}$	$\frac{k_1(a)}{Pa^{\beta}}$
8	0.2802	0.2769	0.2833	0.2696	0.2885	0.2615	0.2926
2	0.3038	0.3025	0.3048	0.2991	0.3060	0.2949	0.3062
1	0.3183	0.3182	0.3182	0.3171	0.3171	0.3151	0.3151
1/2	0.3355	0.3366	0.3341	0.3382	0.3305	0.3386	0.3261
1/8	0.3813	0.3855	0.3768	0.3933	0.3673	0.3999	0.3572

7. Results and discussion

Tables 1 and 2 show some examples for the stress intensity factors obtained for a flat stamp (Fig. 3) by assuming that $a/h = 0.1, 0.5$; $\eta = 0, 0.1, 0.3, 0.5$ and $\nu = 0.3$. In these examples the variable is assumed to be the stiffness ratio $\Gamma_3 = \mu_2/\mu_1$ (Fig. 3). The tables also give the powers of stress singularity, β and α, respectively at the leading ($x = -a$) and the trailing ($x = a$) ends of the stamp corresponding to $\nu = 0.3$ and

Table 2
Stress intensity factors for flat stamp $a/h = 0.5$, $\Gamma_3 = \mu_2/\mu_1$ (Fig. 3)

	$\eta = 0.0$, $\alpha = -0.5$, $\beta = -0.5$	$\eta = 0.1$, $\alpha = -0.5091$, $\beta = -0.4909$		$\eta = 0.3$, $\alpha = -0.5272$, $\beta = -0.4728$		$\eta = 0.5$, $\alpha = -0.5452$, $\beta = -0.4548$	
Γ_3	$\frac{k_1(a)}{Pa^\beta}$	$\frac{k_1(-a)}{Pa^\alpha}$	$\frac{k_1(a)}{Pa^\beta}$	$\frac{k_1(-a)}{Pa^\alpha}$	$\frac{k_1(a)}{Pa^\beta}$	$\frac{k_1(-a)}{Pa^\alpha}$	$\frac{k_1(a)}{Pa^\beta}$
8	0.2086	0.1973	0.2199	0.1754	0.2422	0.1549	0.2635
2	0.2700	0.2657	0.2740	0.2565	0.2814	0.2467	0.2876
1	0.3183	0.3182	0.3182	0.3171	0.3171	0.3151	0.3151
1/2	0.3848	0.3895	0.3800	0.3979	0.3696	0.4053	0.3587
1/8	0.6011	0.6178	0.5844	0.6510	0.5511	0.6834	0.5185

Table 3
Stress intensity factors for the triangular stamp $b/h = 0.2$, $\Gamma_3 = \mu_2/\mu_1$ (Fig. 4)

	$\eta = 0.0$, $\alpha = +0.5$, $\beta = -0.5$	$\eta = 0.1$, $\alpha = +0.4909$, $\beta = -0.4909$	$\eta = 0.3$, $\alpha = +0.4728$, $\beta = -0.4728$	$\eta = 0.5$, $\alpha = +0.4548$, $\beta = -0.4548$
Γ_3	$\frac{k_1(0)}{\mu_1 mb^\alpha}$	$\frac{k_1(0)}{\mu_1 mb^\alpha}$	$\frac{k_1(0)}{\mu_1 mb^\alpha}$	$\frac{k_1(0)}{\mu_1 mb^\alpha}$
8	1.6247	1.6430	1.6751	1.7005
2	1.4976	1.5041	1.5128	1.5160
1	1.4286	1.4280	1.4234	1.4142
1/2	1.3550	1.3467	1.3279	1.3063
1/8	1.1912	1.1677	1.1224	1.0789

Table 4
Stress intensity factors for the triangular stamp $b/h = 0.5$, $\Gamma_3 = \mu_2/\mu_1$ (Fig. 4)

	$\eta = 0.0$, $\alpha = +0.5$, $\beta = -0.5$	$\eta = 0.1$, $\alpha = +0.4909$, $\beta = -0.4909$	$\eta = 0.3$, $\alpha = +0.4728$, $\beta = -0.4728$	$\eta = 0.5$, $\alpha = +0.4548$, $\beta = -0.4548$
Γ_3	$\frac{k_1(0)}{\mu_1 mb^\alpha}$	$\frac{k_1(0)}{\mu_1 mb^\alpha}$	$\frac{k_1(0)}{\mu_1 mb^\alpha}$	$\frac{k_1(0)}{\mu_1 mb^\alpha}$
8	2.1922	2.2358	2.3188	2.3951
2	1.6876	1.6976	1.7132	1.7228
1	1.4286	1.4280	1.4234	1.4142
1/2	1.1794	1.1736	1.1593	1.1418
1/8	0.7522	0.7470	0.7347	0.7203

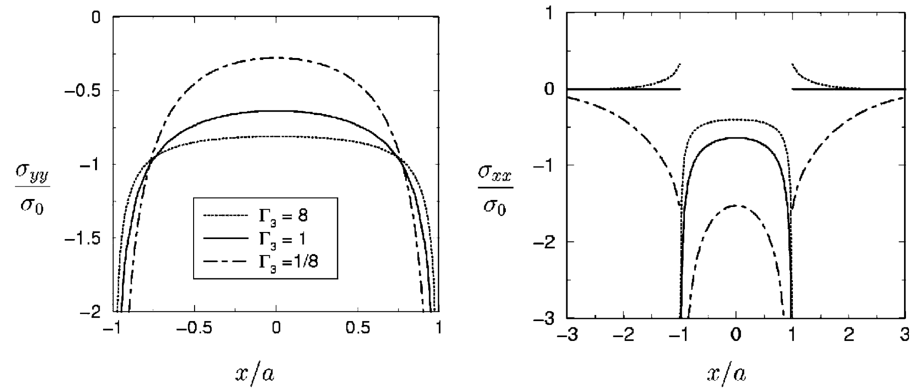

Fig. 5. Stress distribution on the surface of the FGM coating loaded by a flat stamp for various values of the stiffness ratio, $\Gamma_3 = \mu_2/\mu_1$, $a/h = 0.5$, $\eta = 0.0$.

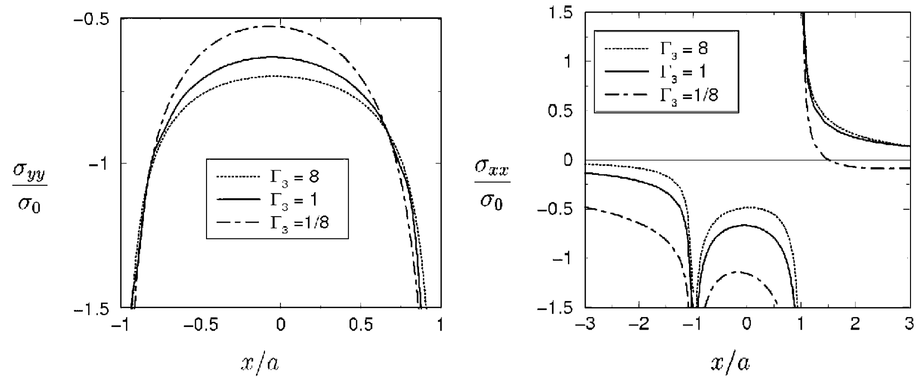

Fig. 6. Stress distribution on the surface of the FGM coating for various values of the stiffness ratio, $\Gamma_3 = \mu_2/\mu_1$, $a/h = 0.1$, $\eta = 0.3$.

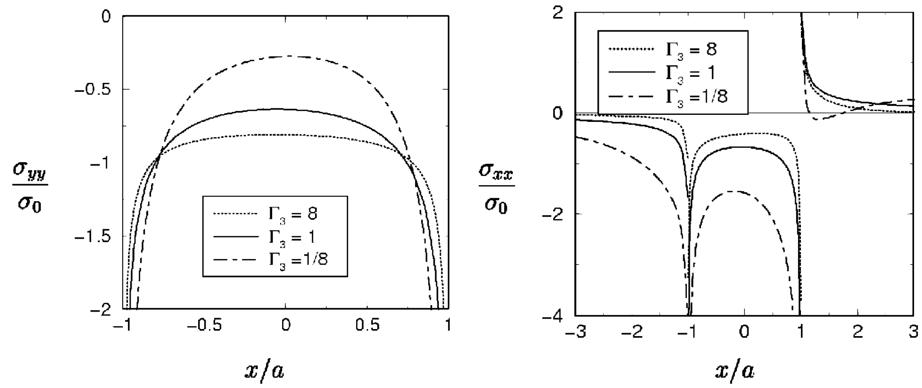

Fig. 7. Stress distribution on the surface of the FGM coating for various values of the stiffness ratio, $\Gamma_3 = \mu_2/\mu_1$, $a/h = 0.5$, $\eta = 0.3$.

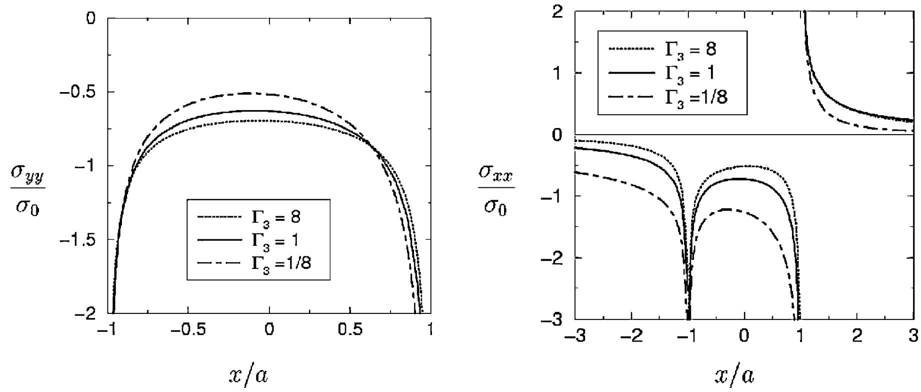

Fig. 8. Stress distribution on the surface of the FGM coating for various values of the stiffness ratio, $\Gamma_3 = \mu_2/\mu_1$, $a/h = 0.1$, $\eta = 0.5$.

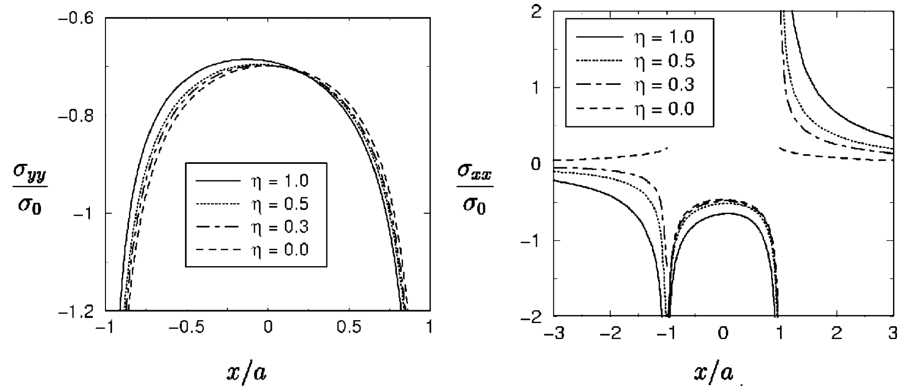

Fig. 9. Stress distribution on the surface of the FGM coating for various values of the coefficient of friction η, $\Gamma_3 = \mu_2/\mu_1 = 8$, $a/h = 0.1$, $\eta = 0.5$.

various values of η. It should be strongly emphasized that in contact problems α and β are independent of the material inhomogeneity parameter (in this case, γ) and depend only on the coefficient of friction η and the value of the Poisson's ratio ν on the surface $y = 0$. The table also shows that the singularity at the trailing end of the stamp is stronger than that at the leading end, i.e., $|\alpha| > |\beta|$. From the tables it may be observed that for stiffer substrates, that is for $\mu_2 > \mu_1$ the stress intensity factors are smaller than that for $\mu_2 < \mu_1$. Tables 3 and 4 show the stress intensity factors and the singularities α and β for a triangular stamp. These tables, too, show greater "stress concentration" at the trailing end relative to the corresponding frictionless stamp.

By examining stress singularities α and β (for example, for the flat stamp) given by (53a) and (54), it may be seen that for a fixed value of κ, as η approaches zero, $\theta \to \pi/2$, $\alpha \to -1/2$, and $\beta \to -1/2$, giving the known square-root singularity for the frictionless sliding stamp. Similarly, as η becomes very large, $\theta \to 0$, $\alpha \to -1$, and $\beta \to 0$. As a consequence the singularity at the trailing end ($x = a$) of the flat stamp becomes stronger and that at the leading end ($x = -a$) becomes weaker than the corresponding singularities for the frictionless stamp.

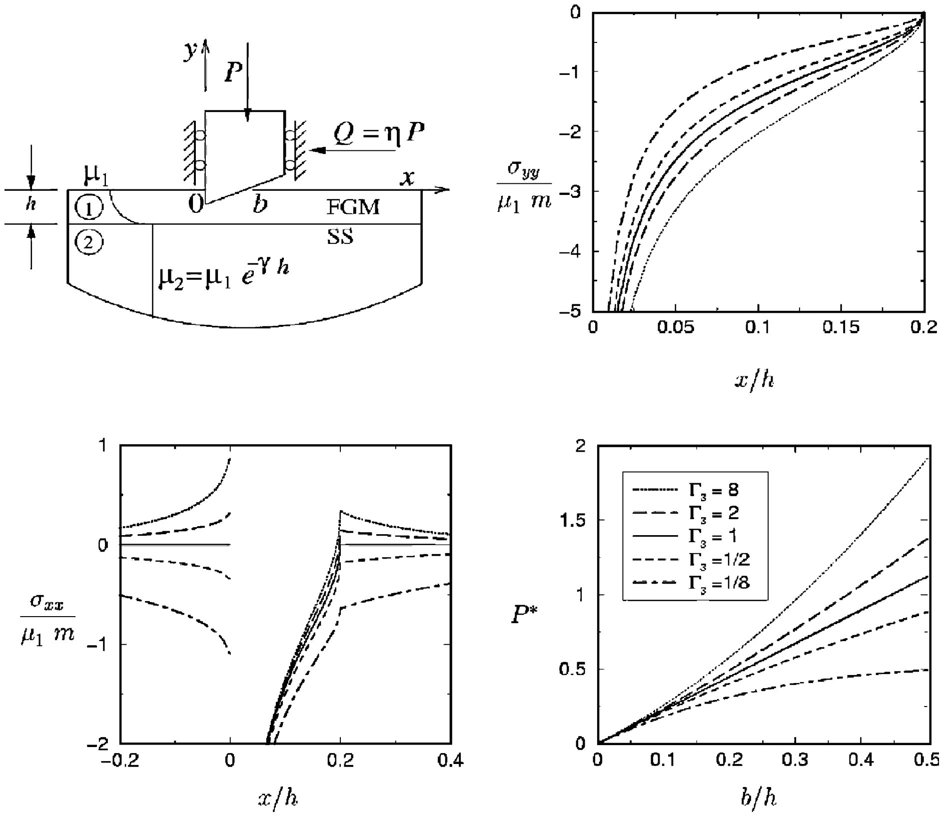

Fig. 10. Stress distribution on the surface of an FGM coating loaded by a rigid triangular stamp for various values of the stiffness ratio, $\Gamma_3 = \mu_2/\mu_1$, $b/h = 0.2$, $\eta = 0$, $P^* = P/(\mu_1 mh)$.

Stress distributions perhaps of greatest practical interest are the contact stress $\sigma_{yy}(x,0)$ (with $\sigma_{xy}(x,0) = \eta\sigma_{yy}(x,0)$) and the in-plane stress $\sigma_{xx}(x,0)$. Any other stress or displacement component may be determined by using the appropriate Green's functions obtained from Fig. 1 and the density functions $p(x)$ and $\eta p(x)$. Figs. 5–9 show some flat stamp results for the stress components on the surface of the FGM coating for various values of the stiffness ratio $\Gamma_3 = \mu_2/\mu_1$ and fixed values of a/h and η. For reference Fig. 5 shows an example for the frictionless flat stamp. Note that the stress distribution is symmetric with respect to the $x = 0$ plane, for $|x| < a$, $\sigma_{xx}(x,0)$ is compressive, for $|x| > a$, $\sigma_{xx} = 0$ for $\Gamma_3 = 1$ (homogeneous half plane), $\sigma_{xx} > 0$ for $\Gamma_3 > 1$ and $\sigma_{xx} < 0$ for $\Gamma_3 < 1$. For $|x| < a$ all stress components become unbounded as $|x| \to a$.

Figs. 6–9 show the influence of the stiffness ratio, Γ_3 the length parameter a/h and the coefficient of friction η on the distribution of $\sigma_{yy}(x,0)$ and $\sigma_{xx}(x,0)$. The most important result is that in the presence of friction $\sigma_{xx}(x,0)$ become positive and unbounded as $x \to a + 0$. Figs. 10–17 show some sample results for a triangular stamp. Specifically, the figures show the effect of the stiffness ratio Γ_3 on $\sigma_{yy}(x,0)$, $\sigma_{xx}(x,0)$ and the resultant force P vs the contact length b relationship for certain combination of b/h and η. Again, for reference the frictionless case is shown in Fig. 10. As expected, because of the singularity, $\sigma_{yy}(x,0)$ and $\sigma_{xx}(x,0)$ become unbounded as $x \to 0$. In this problem the length b describing the location of the smooth contact is unknown and is a monotonically increasing, highly nonlinear function of P. The problem is solved by assuming b, then computing P from the static equilibrium of the stamp. P vs. b given in the figures

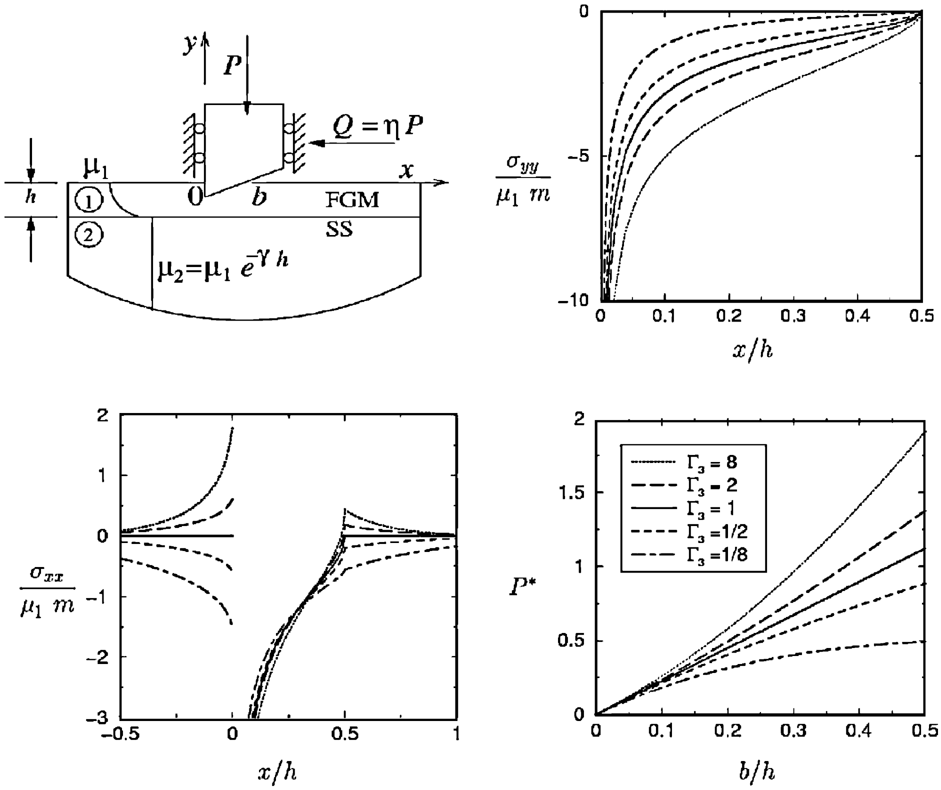

Fig. 11. Stress distribution on the surface of an FGM coating loaded by a rigid triangular stamp for various values of the stiffness ratio, $\Gamma_3 = \mu_2/\mu_1$, $b/h = 0.5$, $\eta = 0$, $P^* = P/(\mu_1 m h)$.

is obtained by repeating this process. The slope m of the stamp has no influence on the singularities. Hence, its influence on the calculated stresses is largely quantitative. One of the more interesting results that may be observed in the triangular stamp problem is the tensile spike in the distribution of $\sigma_{xx}(x,0)$ as $x \to b$ which, clearly, has some implications regarding the initiation and subcritical growth of surface cracks under repeated loading. Another interesting result that may be observed from Figs. 16 and 17 is that fixing Γ_3 and b/h and varying η seem to have almost no influence on $\sigma_{yy}(x,0)$ but rather significant effect on $\sigma_{xx}(x,0)$.

As pointed out previously, in the sliding contact problem under consideration the weight functions $w(x)$ and, consequently, the singularities of contact stresses are dependent on the coefficient of friction η and the surface value of the Poisson's ratio v (or the material parameter κ) only, and are independent of all material constants (such as γ, μ_1 and μ_2 (see Eqs. (1) and (2)) and length parameters (such as h, a, b and m) (see Figs. 3 and 4). Also, observing that on physical grounds the surface value of the shear modulus μ_1 must be nonzero, the leading term in the asymptotic solution of the general sliding contact problem described in Fig. 1 may be obtained by assuming that the coating thickness h tends to infinity and, as a result γ tends to zero, η is a known constant and the medium is homogeneous with elastic properties μ_1 and κ. The closed form solutions for the two stamp geometries considered in this study, namely the flat and triangular stamps are given in Appendix A. The results shown in the Appendix A include the contact stresses $\sigma_{yy}(x,0)$, $\sigma_{xy}(x,0) = \eta\sigma_{yy}(x,0)$, the in-plane stress $\sigma_{xx}(x,0)$, and the stress intensity factors $k_1(\pm a)$, or $k_1(0)$. The singular behavior of the asymptotic solution given in the Appendix A is thus identical to that of the actual

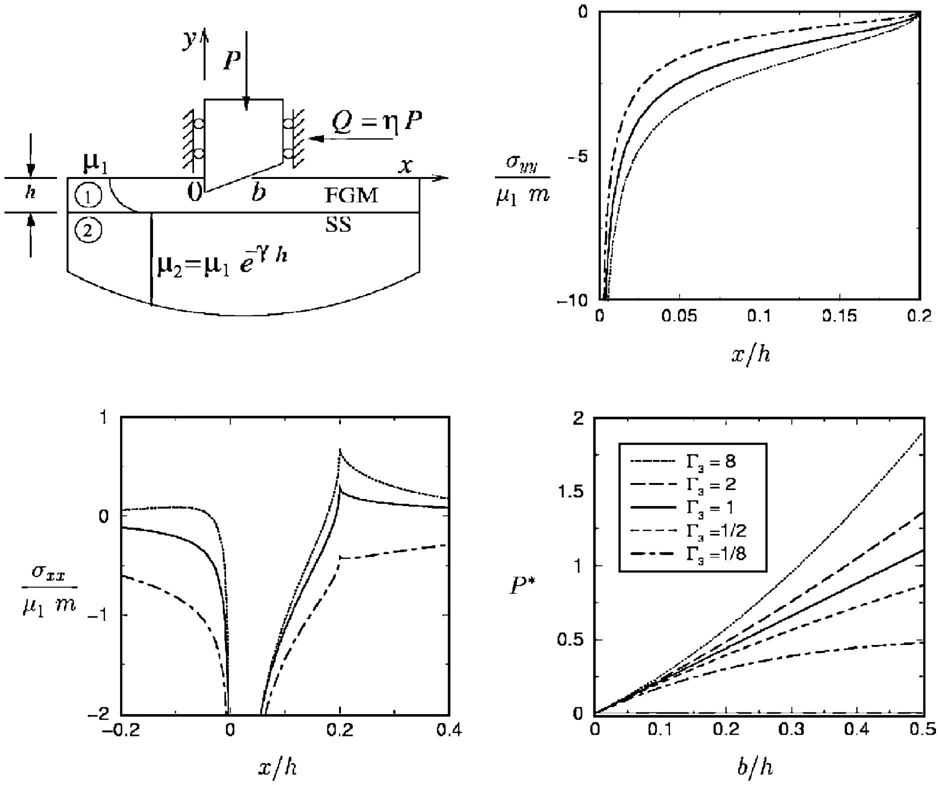

Fig. 12. Stress distribution on the surface of an FGM coating loaded by a rigid triangular stamp for various values of the stiffness ratio, $\Gamma_3 = \mu_2/\mu_1$, $b/h = 0.2$, $\eta = 0.1$, $P^* = P/(\mu_1 mh)$.

problems described in Figs. 3 and 4. The difference is in the multiplying factors such as the stress intensity factors (see Eqs. (66a), (66b), (80), (A.6), (A.7) and (A.13) and Tables 1–4).

8. Some concluding remarks

In sliding contact problems for graded materials the weight functions describing the asymptotic behavior of the contact stresses are dependent, as in the homogeneous materials, on the coefficient of friction and the surface value of the Poisson's ratio only, and are independent of all other material constants and length parameters. Thus, the leading term in the asymptotic solution of the general sliding contact problem for graded coatings may be obtained from the corresponding homogeneous half plane solution which, for many simplified stamp geometries, may be evaluated in closed form. Generally at the trailing end of the contact area the "stress concentration" is higher than that at the leading end. For example, for a flat stamp $|\alpha| > |\beta|$, $\alpha < 0$, $\beta < 0$, α and β being the power of stress singularity at the trailing and the leading end of the stamp, respectively.

The results indicate that in sliding contact problems for graded coatings the influence of not only the coefficient of friction(which is expected) but also the material inhomogeneity constant γ or the stiffness ratio Γ_3 on the contact stresses, particularly the stress intensity factors can be quite significant.

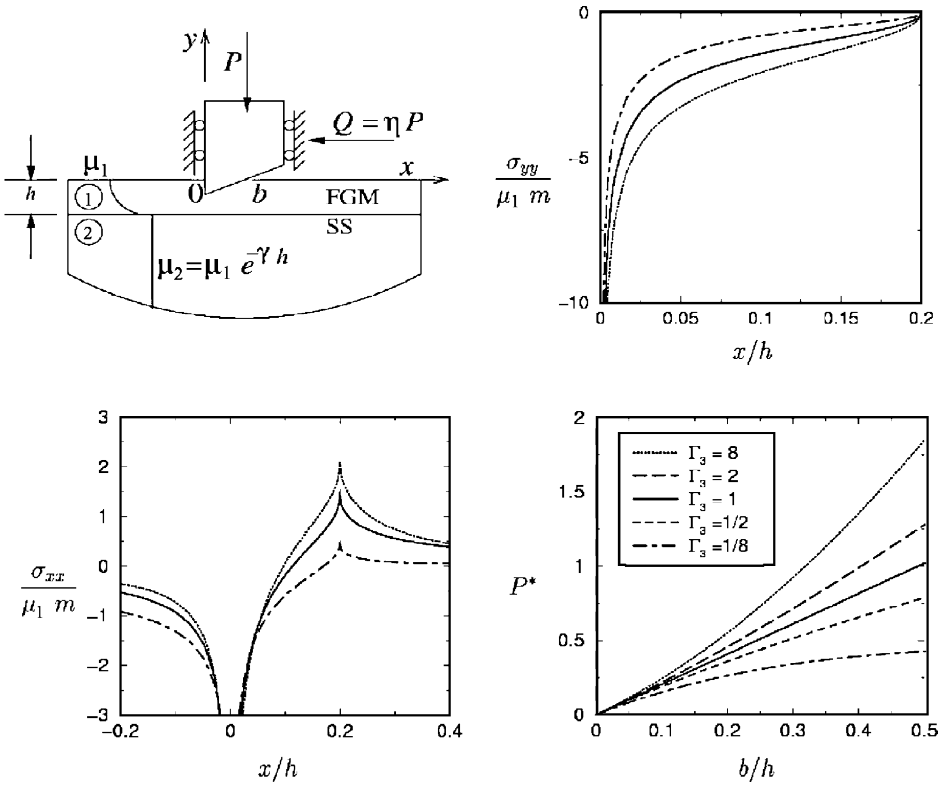

Fig. 13. Stress distribution on the surface of an FGM coating loaded by a rigid triangular stamp for various values of the stiffness ratio, $\Gamma_3 = \mu_2/\mu_1$, $b/h = 0.2$, $\eta = 0.5$, $P^* = P/(\mu_1 m h)$.

Acknowledgement

This work was partially supported by Air Force Office of Scientific Research under the grant F49620-98-1-0028.

Appendix A

Closed form solution for a rigid flat stamp on a homogeneous half space may be obtained as (Guler, 2001)

$$\frac{\sigma_{yy}(x,0)}{\sigma_0} = \frac{2\sin\pi\alpha}{\pi}\left(1-\frac{x}{a}\right)^{\alpha}\left(1+\frac{x}{a}\right)^{\beta}, \tag{A.1}$$

$$\frac{\sigma_{xx}(x,0)}{\sigma_0} = \frac{2\sin\pi\alpha}{\pi}\begin{cases}\left(1-\frac{x}{a}\right)^{\alpha}\left(1+\frac{x}{a}\right)^{\beta} + \frac{2\eta}{\pi}L_f(x), & -a < x < a,\\ \dfrac{2\eta}{\pi}L_f(x), & |x| > a,\end{cases} \tag{A.2}$$

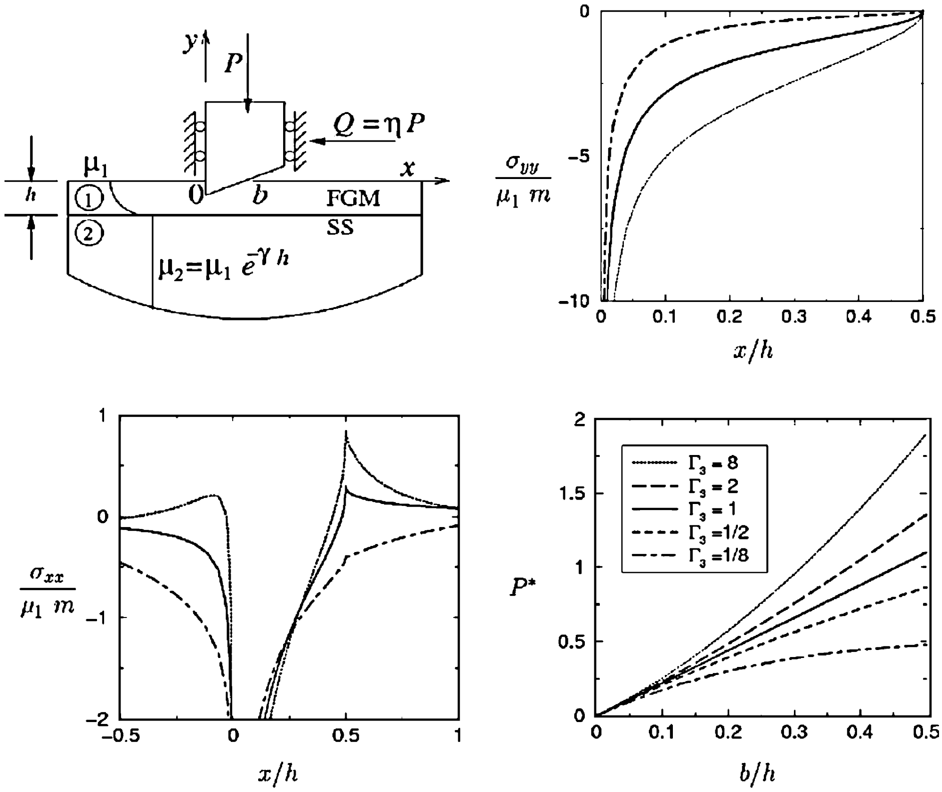

Fig. 14. Stress distribution on the surface of an FGM coating loaded by a rigid triangular stamp for various values of the stiffness ratio, $\Gamma_3 = \mu_2/\mu_1$, $b/h = 0.5$, $\eta = 0.1$, $P^* = P/(\mu_1 mh)$.

where

$$L_f(x) = \frac{\pi}{\sin \pi\alpha} \begin{cases} \left(1-\frac{x}{a}\right)^{\alpha}\left(1+\frac{x}{a}\right)^{\beta}, & -\infty < x < -a, \\ \left(1-\frac{x}{a}\right)^{\alpha}\left(1+\frac{x}{a}\right)^{\beta}\cos \pi\alpha, & -a < x < a, \\ \left(\frac{x}{a}-1\right)^{\alpha}\left(1+\frac{x}{a}\right)^{\beta}, & a < x < \infty, \end{cases} \tag{A.3}$$

$$\sigma_0 = \frac{P}{2a}, \tag{A.4}$$

$$\alpha = -1 + \frac{\theta}{\pi}, \quad \beta = -\frac{\theta}{\pi}, \quad \theta = \arctan\left|\frac{\kappa+1}{\eta(\kappa-1)}\right|. \tag{A.5}$$

The stress intensity factors at the ends of the flat stamp can be found from

$$k_1(a) = -\frac{2\sigma_0}{\pi a^{\alpha}} \sin \pi\alpha, \tag{A.6}$$

$$k_1(-a) = -\frac{2\sigma_0}{\pi a^{\beta}} \sin \pi\alpha. \tag{A.7}$$

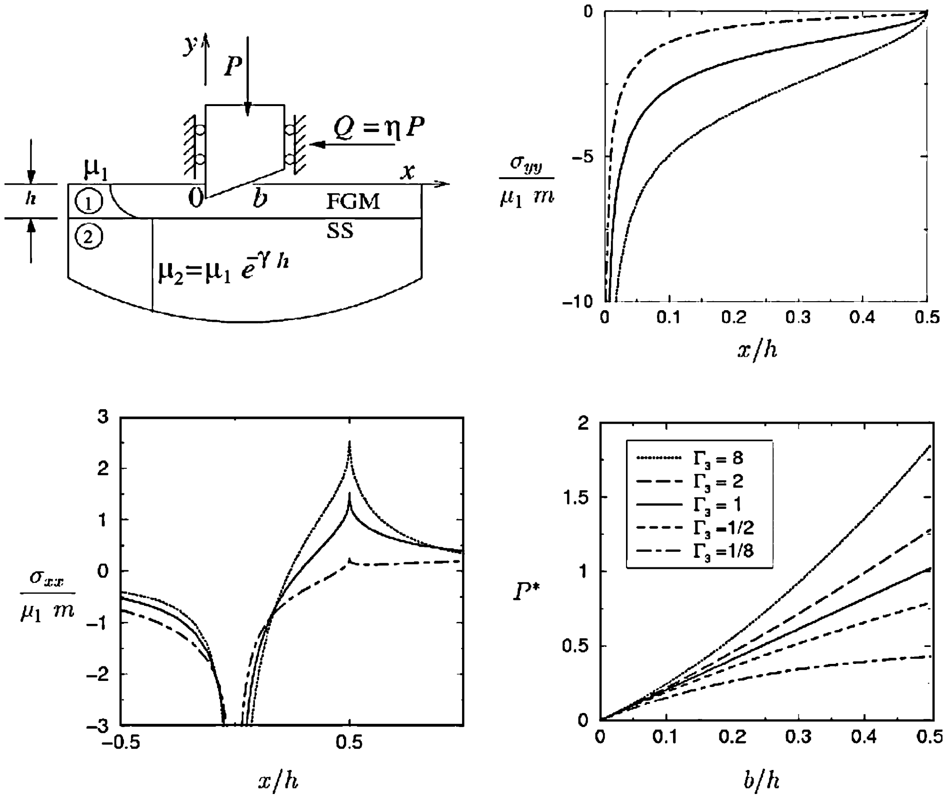

Fig. 15. Stress distribution on the surface of an FGM coating loaded by a rigid triangular stamp for various values of the stiffness ratio, $\Gamma_3 = \mu_2/\mu_1$, $b/h = 0.5$, $\eta = 0.5$, $P^* = P/(\mu_1 m h)$.

Closed form solution of the triangular stamp can be obtained as (Guler, 2001)

$$\frac{\sigma_{yy}(x,0)}{\mu_1 m} = -\frac{4}{\kappa+1}\sin\pi\alpha\left(\frac{b-x}{x}\right)^{\alpha}, \tag{A.8}$$

$$\frac{\sigma_{xx}(x,0)}{\mu_1 m} = -\frac{4\sin\pi\alpha}{\kappa+1}\begin{cases}\left(\dfrac{b-x}{x}\right)^{\alpha} + \dfrac{2\eta}{\pi}L_t(x), & 0 < x < b,\\[2mm] \dfrac{2\eta}{\pi}L_t(x), & x < 0,\ x > b,\end{cases} \tag{A.9}$$

where

$$L_t(x) = \frac{\pi}{\sin\pi\alpha}\begin{cases}-\left(\dfrac{x-b}{x}\right)^{\alpha} - 1, & x < 0,\\[2mm] \left(\dfrac{b-x}{x}\right)^{\alpha}\cos\pi\alpha - 1, & 0 < x < b,\\[2mm] \left(\dfrac{x-b}{x}\right)^{\alpha}, & x > b.\end{cases} \tag{A.10}$$

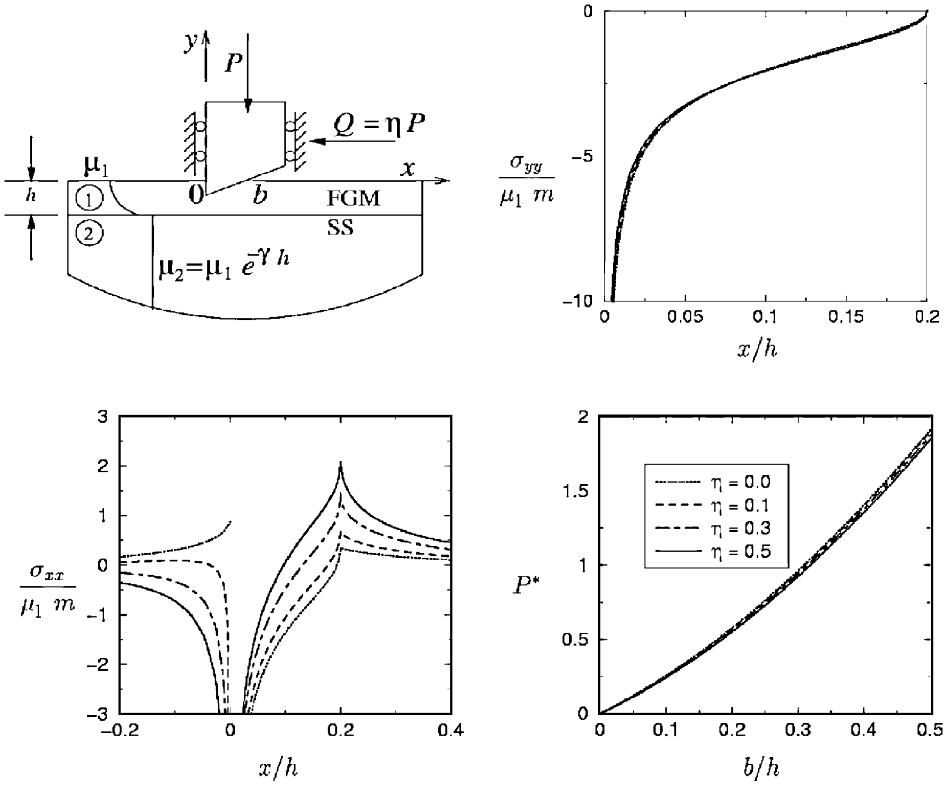

Fig. 16. Stress distribution on the surface of an FGM coating loaded by a rigid triangular stamp for various values of the coefficient of friction η, $\Gamma_3 = \mu_2/\mu_1 = 8$, $b/h = 0.2$, $P^* = P/(\mu_1 mh)$.

$$\alpha = \frac{\theta}{\pi}, \quad \beta = -\frac{\theta}{\pi}, \quad \theta = \arctan\left|\frac{\kappa+1}{\eta(\kappa-1)}\right|. \tag{A.11}$$

The load versus contact length relation may be expressed as

$$\frac{P}{\mu_1 m} = \frac{4\pi\alpha}{\kappa+1} b. \tag{A.12}$$

The stress intensity factor at the sharp end of the triangular stamp is found to be

$$k_1(0) = \frac{4\mu_1 m b^{\alpha}}{\kappa+1} \sin \pi\alpha. \tag{A.13}$$

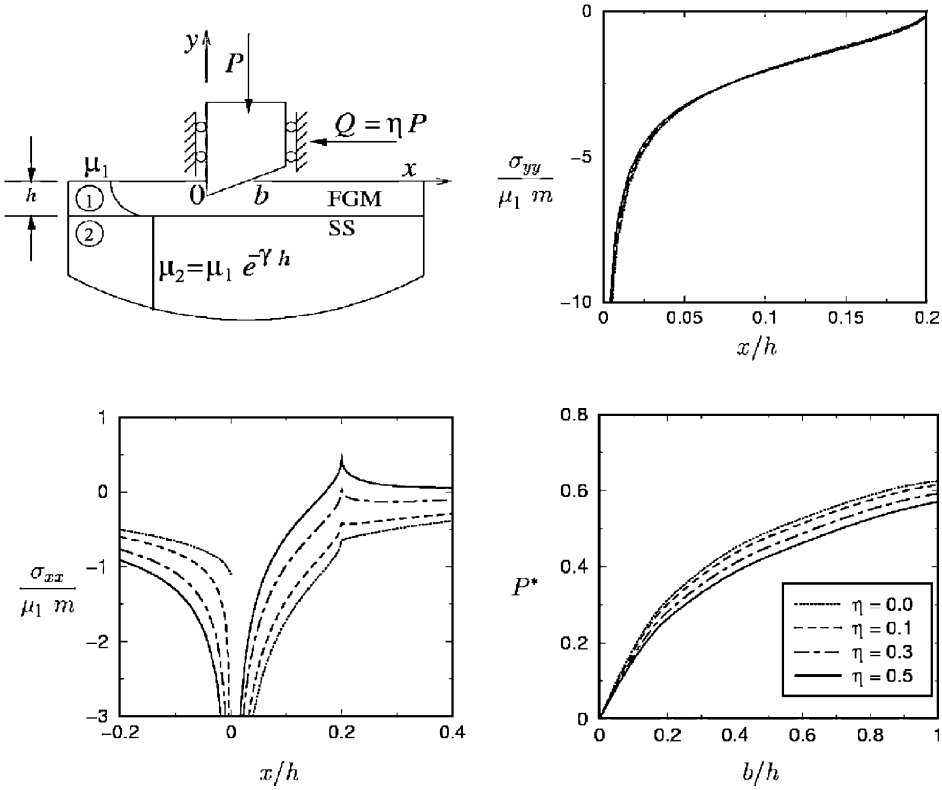

Fig. 17. Stress distribution on the surface of an FGM coating loaded by a rigid triangular stamp for various values of the coefficient of friction η, $\Gamma_3 = \mu_2/\mu_1 = 1/8$, $b/h = 0.2$, $P^* = P/(\mu_1 mh)$.

References

Booker, J.R., Balaam, N.P., Davis, E.H., 1985. The behavior of an elastic nonhomogeneous half space. Part I: Line and point loads. Part II: Circular and strip footings. Int. J. Numer. Anal. Meth. Geomech. 9, 353–381.

Ciavarella, M., 1998a. The generalized Cattaneo partial slip plane contact problem. I—theory. Int. J. Solids Struct. 35 (18), 2349–2362.

Ciavarella, M., 1998b. The generalized Cattaneo partial slip plane contact problem. II—examples. Int. J. Solids Struct. 35 (18), 2363–2378.

Dag, S., Erdogan, F., 2002. A surface crack in a graded medium loaded by a rigid stamp. Engng. Fract. Mech. 69, 1729–1751.

Erdogan, F., Gupta, G.D., 1972. On the numerical solution of singular integral equations. Quart. Appl. Math. 29, 525–534.

Giannakopoulos, A., Suresh, S., 1997a. Indentation of solids with gradients in elastic properties: Part I. Point force solution. Int. J. Solids Struct. 34 (19), 2357–2392.

Giannakopoulos, A., Suresh, S., 1997b. Indentation of solids with gradients in elastic properties: Part II. Axisymetric indenters. Int. J. Solids Struct. 34 (19), 2393–2428.

Giannakopoulos, A.E., Pallot, P., 2000. Two-dimensional contact analysis of elastic graded materials. J. Mech. Phys. Solids 48, 1597–1631.

Guler, M.A., 2001. Contact Mechanics of FGM Coatings, Ph.D. Dissertation, Lehigh University.

Guler, M.A., Erdogan, F., 1998. Contact mechanics of FGM coatings. In: Newaz, G.M., Gibson, R.F. (Eds.), Proceedings of 8th Japan—US Conference on Composite Materials, pp. 397–408.

Hills, D.A., Nowell, D., Sackfield, A., 1993. Mechanics of Elastic Contacts. Butterworth, Heinemann, Oxford.

Lawn, B.R., 1993. Fracture of Brittle Solids, 2nd ed. Cambridge University Press, Cambridge, UK.

Miyamoto, M., Kaysser, W.A., Rabin, B.H., Kawasaki, A., Ford, R.G. (Eds.), 1999. Functionally Graded Materials: Design, Processing and Applications. Kluwer Academic Publishers, Norwell, MA.

Muskhelishvili, N.L., 1953. Singular Integral Equations. P. Noordhoff, Groningen, The Netherlands.

Pan, W., Gong, J., Zhang, L., Chen, L. (Eds.), 2003. Functionally Graded Materials VII. Trans Tech Publications Ltd., Switzerland.
Suresh, S., Giannakopoulos, A.E., Alcala, J., 1997. Spherical indentation of compositionally graded materials: theory and experiments. Acta Mater. 45 (4), 1307–1321.
Suresh, S., Olsson, M., Giannakopoulos, A.E., Padture, N.P., Jitcharoen, J., 1999. Engineering the resistance to sliding-contact damage through controlled gradients in elastic properties at contact surfaces. Acta Mater. 47 (14), 3915–3926.
Trumble, K., Bowman, K., Reimanis, I., Sampath, S. (Eds.), 2000. Functionally Graded Materials 2000, Ceramic Transactions, vol. 114, The American Ceramic Society, Westerville, Ohio 43081.